Available online at www.sciencedirect.com
SCIENCE DIRECT®
Journal of Magnetic Resonance 173 (2005) 116–124
JMR Journal of Magnetic Resonance
www.elsevier.com/locate/jmr

Optimal experiments for maximizing coherence transfer between coupled spins☆

Navin Khaneja[a,*], Frank Kramer[b], Steffen J. Glaser[b]

[a] Division of Engineering and Applied Sciences, Harvard University, Cambridge, MA 02138, USA
[b] Department of Chemistry, Technische Universität München, 85747 Garching, Germany

Received 7 October 2004; revised 18 November 2004
Available online 19 December 2004

Abstract

In spite of great advances in the theory and applications of magnetic resonance in the past 50 years, some basic questions in spin physics have not yet been answered. In the absence of relaxation losses, what is the maximum amount of coherence that can be transferred between coupled spins under general coupling tensors in a given time and how can this be realized experimentally? Since transfer of coherence between spins forms the basis for multidimensional experiments in NMR spectroscopy, the answers to these questions are of both practical and theoretical interest. Computing the physical limits of coherence transfer involves characterizing all unitary evolutions that can be synthesized in a given time. Here we derive these limits and show how they can be achieved experimentally.

Keywords: Coherence transfer; Transfer efficiency; Time optimal pulse sequences; General coupling tensors; Multidimensional NMR

1. Introduction

Determining how close a quantum mechanical system can be driven from a given initial state to a desired target state in a specified amount of time is an important practical problem. This problem arises in the areas of coherent spectroscopy and control of quantum systems where one actively manipulates quantum dynamics through tailored electromagnetic fields. However, in most applications, external controls alone are not sufficient to bring the system to a desired target state. Evolution under the internal Hamiltonian is essential to move between quantum mechanical states of interest. For example, in NMR spectroscopy, appropriate combinations of external excitation through radio-frequency (rf) pulses and evolution under couplings between nuclear spins is used to steer a spin system to a target state, e.g., to transfer coherence from one spin to another. The necessity of having the spin system evolve under its internal Hamiltonian puts physical limits on the minimum time it takes to transfer coherence between coupled spins and on the maximum coherence that can be transferred in a specified time. Minimizing this time for coherence transfer does not necessarily minimize relaxation losses [25,27]. However, in the absence of a detailed knowledge of relaxation rates and mechanisms, reducing relaxation losses by finding the shortest possible pulse sequence is a practical approach.

Until now, the limits of coherence transfer between coupled spins in a specified time were unknown. In this paper, we solve this problem for general coupling tensors and find optimal pulse sequences for achieving optimal coherence transfer. This problem is solved under the assumption that the coupled spins under consideration

☆ This work was funded by AFOSR Grant FA9550-04-1-0427, NSF 0133673, and NSF 0218411 and Deutsche Forschungsgemeinschaft under Grant Gl 203/4-2.
* Corresponding author. Fax: +1 617 4952809.
E-mail address: navin@hrl.harvard.edu (N. Khaneja).

1090-7807/$ - see front matter © 2004 Elsevier Inc. All rights reserved.
doi:10.1016/j.jmr.2004.11.023

can be selectively manipulated at rates faster than the coupling evolution. To compute these limits and the optimal pulse sequences, we make use of an explicit characterization of the set of all unitary propagators that can be synthesized in a given time [1,2]. We also provide experimental data which shows how these methods can be used to improve sensitivity of current NMR experiments when the time for coherent evolution is restricted. Finally, we discuss how these methods might be generalized to larger spin systems and other applications involving control of quantum dynamics.

2. Theory

We consider a pair of coupled spins, where the coupling Hamiltonian $\mathscr{H}_c$ has the form

$$\mathscr{H}_c = 2\pi C(\mu_1 I_x S_x + \mu_2 I_y S_y + \mu_3 I_z S_z), \tag{1}$$

where $|\mu_3| \geqslant |\mu_2| \geqslant |\mu_1|$.

Note that the above form of the coupling Hamiltonian is completely general as any coupling term of the form

$$\mathscr{H}_c = 2\pi \sum_{\alpha,\beta} I_\alpha C_{\alpha\beta} S_\beta = 2\pi\, \mathbf{I}\, \mathbf{C}\, \mathbf{S}$$

with arbitrary real elements $C_{\alpha\beta}$ can be transformed to the form given in Eq. (1) by local unitary transformations on the two spins [2]. By local unitary transformations we mean unitary evolutions produced by spin selective excitations.

To see this, observe that by *singular value decomposition* of the general coupling tensor $\mathbf{C}$, we can choose three-dimensional rotations (with possibly negative determinant) such that $\Theta_1 \mathbf{C} \Theta_2$ is diagonal with non-negative entries. By local unitary transformations, we can transform the coupling tensor $\mathbf{C} \to U\mathbf{C}V$, where U, V are three-dimensional rotations with positive determinant, reflecting rotations on spin I and S, respectively. Now U and V can be chosen so that

$$U\mathbf{C}V = C \begin{bmatrix} \mu_1 & 0 & 0 \\ 0 & \mu_2 & 0 \\ 0 & 0 & \mu_3 \end{bmatrix},$$

where $|\mu_3| \geqslant |\mu_2| \geqslant |\mu_1|$ and μ_i are either all positive or all negative (not both).

We assume that the two spins under consideration can be selectively manipulated at rates faster than the coupling evolution, which is always possible if the frequency difference between the spins is much larger than the strength of coupling Hamiltonian. This allows us to produce any local unitary transformation in a time during which there is negligible evolution under the coupling Hamiltonian. Under these assumptions, the following theorem completely characterizes the unitary transformations that can be achieved in any given time t [1,2].

Theorem 1. [1,2] *Let* $\mathscr{H}_c = 2\pi C(\mu_1 I_x S_x + \mu_2 I_y S_y + \mu_3 I_z S_z)$ *be the coupling Hamiltonian for a system consisting of two spins* 1/2. *Any unitary transformation* U *on two spins can be represented as* $U = K_1 A K_2$, *where* K_1 *and* K_2 *are local unitary transformations and* A *is a non-local unitary transformation of the form* $\exp\{-\mathrm{i}(a_x I_x S_x + a_y I_y S_y + a_z I_z S_z)\}$. *All unitary transformations* $U(t)$ *that can be synthesized in time* t *have the form*

$$U(t) = K_1 \exp\{-\mathrm{i}2\pi C t(\alpha I_x S_x + \beta I_y S_y + \gamma I_z S_z)\} K_2. \tag{2}$$

Here (α, β, γ) lies in the convex cone generated by vectors (μ_1, μ_2, μ_3), $(\mu_1, -\mu_2, -\mu_3)$, $(-\mu_1, -\mu_2, \mu_3)$, and $(-\mu_1, \mu_2, -\mu_3)$ and their various permutations, e.g., (μ_1, μ_3, μ_2) is a permutation of (μ_1, μ_2, μ_3). K_1 and K_2 are arbitrary local unitary transformations. A vector x belongs to the cone of vectors $\{y_i\}$ if $x = \sum_i \alpha_i y_i$, where $\alpha_i \geqslant 0$ and $\sum_i \alpha_i \leqslant 1$.

It is straightforward to see that any unitary transformation in Eq. (2) can be achieved in time t. Starting from the Hamiltonian of the form $\mu_1 I_x S_x + \mu_2 I_y S_y + \mu_3 I_z S_z$, by a 90°_x rotation on both spins, we can prepare the effective Hamiltonian $\mu_1 I_x S_x + \mu_3 I_y S_y + \mu_2 I_z S_z$. Similarly, by a selective 180°_x rotation on one of the spins, we can also prepare the effective Hamiltonian $\mu_1 I_x S_x - \mu_2 I_y S_y - \mu_3 I_z S_z$. Now it is clear that by a series of such double and selective rotations any Hamiltonian of the form $pI_x S_x + qI_y S_y + rI_z S_z$ can be synthesized, where (p, q, r) is one of (μ_1, μ_2, μ_3), $(\mu_1, -\mu_2, -\mu_3)$, $(-\mu_1, -\mu_2, -\mu_3)$, $(-\mu_1, \mu_2, -\mu_3)$ or their permutations. Since all these Hamiltonians commute, we can, by concatenation of evolution under these transformed Hamiltonians, synthesize an average Hamiltonian $\alpha I_x S_x + \beta I_y S_y + \gamma I_z S_z$, where (α, β, γ) lies in the specified convex cone. Since local unitary transformations are assumed to take negligible time to produce, it is now clear that any U as defined in Eq. (2) can be synthesized. Using convexity results from matrix analysis, it can be shown that these are the only unitary evolutions that can be produced in time t [2].

We now use this theorem to compute the maximum coherence that can be transferred between coupled spins in a specified time t. Let the initial density operator terms of interest be $\rho(0)$ and denote the density operator at time t by $\rho(t) = U(t)\rho(0)U(t)^\dagger$. The efficiency of transfer to a target operator F at time t is defined as [3]

$$\eta(t) = \frac{|\mathrm{tr}(F^\dagger \rho(t))|}{\|F\|\ \|\rho(0)\|}. \tag{3}$$

Result 1: Given the coupling Hamiltonian $\mathscr{H}_c = 2\pi C(\mu_1 I_x S_x + \mu_2 I_y S_y + \mu_3 I_z S_z)$, the maximum efficiency $\eta^*(t)$ of the coherence transfer in time t for $t \leqslant t_{\min}$, and the minimum time $t_{\min}$ for complete transfer for important experiments are summarized in Table 1.

Table 1
Maximum transfer efficiency $\eta^*(t)$ and minimum time $t_{\min}$ for complete transfer

Transfer	$\eta^*(t)$ $(t \leqslant t_{\min})$	$t_{\min}^{-1}$
$I_x \to S_x$	$\sin^2(\frac{\pi}{2}C(\lvert\mu_3\rvert + \lvert\mu_2\rvert)t)$	$C(\lvert\mu_3\rvert + \lvert\mu_2\rvert)$
$I^- \to S^-$	$\sin(\pi Ca)\sin(\pi Cb)$	$\frac{2}{3}C(\lvert\mu_3\rvert + \lvert\mu_2\rvert + \lvert\mu_1\rvert)$
$I_x \to 2I_zS_x$	$\sin(\pi C\lvert\mu_3\rvert t)$	$2C\lvert\mu_3\rvert$
$I^- \to 2I_zS^-$	$\max_x \sin(\frac{\pi}{2}C\{\lvert\mu_3\rvert + \lvert\mu_2\rvert - \lvert\mu_1\rvert + x\}t)\cos(\pi Ctx)$	$C(\lvert\mu_3\rvert + \lvert\mu_2\rvert - \lvert\mu_1\rvert)$
$I_xS_\beta \to I_\beta S_x$	$\sin(\frac{\pi}{2}C(\lvert\mu_3\rvert + \lvert\mu_2\rvert)t)$	$C(\lvert\mu_3\rvert + \lvert\mu_2\rvert)$
$I^-S_\beta \to I_\beta S^-$	$\sin(\frac{\pi}{2}C(\lvert\mu_3\rvert + \lvert\mu_2\rvert)t)$	$C(\lvert\mu_3\rvert + \lvert\mu_2\rvert)$

Note. $I^- = I_x - \mathrm{i}I_y$ and $I_\beta = \frac{1}{2} - I_z$. For the transfer $I^- \to S^-$, the optimal values of a and b are completely characterized by the two conditions $a + 2b = (\lvert\mu_3\rvert + \lvert\mu_2\rvert + \lvert\mu_1\rvert)t$ and $\tan(\pi Ca) = 2\tan(\pi Cb)$.

The proof of the optimal transfer efficiencies $\eta^*(t)$ and minimum times $t_{\min}$ summarized in Table 1 uses the characterization of all the unitary transformations that can be achieved in a given time t as characterized in Eq. (2). For details see Appendix A. Here, we illustrate the basic ideas involved in proving the above relations by considering the first example ($I_x \to S_x$).

For this case, Eq. (3) reduces to

$$\eta(t) = |\mathrm{tr}\{S_xU(t)I_xU^\dagger(t)\}| \tag{4}$$

as $\|I_x\| = \|S_x\| = 1$. We need to find the unitary propagator $U(t)$ that maximizes $\eta(t)$. As explained before, it takes negligible time to synthesize the local unitary transformations K_1 and K_2 in Eq. (2). Let $K_2I_xK_2^\dagger = m_1I_x + m_2I_y + m_3I_z$ and $K_1^\dagger S_xK_1 = n_1S_x + n_2S_y + n_3S_z$, where $\sum_i m_i^2 = 1$ and $\sum_j n_j^2 = 1$. Eq. (4) then can be written as

$$\begin{aligned}\eta(t) = {} & m_1n_1\sin(\pi C\beta t)\sin(\pi C\gamma t) + m_2n_2\sin(\pi C\alpha t)\\ & \times \sin(\pi C\gamma t) + m_3n_3\sin(\pi C\alpha t)\sin(\pi C\beta t),\end{aligned} \tag{5}$$

where (α, β, γ) lies in the convex cone generated by vectors (μ_1, μ_2, μ_3), $(\mu_1, -\mu_2, -\mu_3)$, $(-\mu_1, -\mu_2, \mu_3)$, $(-\mu_1, \mu_2, -\mu_3)$, and their various permutations. If $\beta + \gamma$ is fixed then $\sin(\pi C\beta t)\ \sin(\pi C\gamma t)$ achieves its maximum value at $\beta = \gamma$. Given the restrictions on (α, β, γ) as described above, this maximum value is achieved when $\beta + \gamma = |\mu_2| + |\mu_3|$ and the maximum value is $\sin^2(\frac{\pi}{2}C(|\mu_3| + |\mu_2|)t)$ (cf. red curves in Fig. 1). Similarly the maximum possible value of $\sin(\pi C\alpha t)\ \sin(\pi C\gamma t)$ and $\sin(\pi C\alpha t)\ \sin(\pi C\beta t)$ is also $\sin^2(\frac{\pi}{2}C(|\mu_3| + |\mu_2|)t)$. Therefore , Eq. (5) achieves its maximum for $m_1 = n_1 = 1$ and for $\beta = \gamma = \frac{1}{2}(|\mu_3| + |\mu_2|)$. Thus, the largest value of Eq. (5) is 1 and is achieved at $t_{\min} = \{C(|\mu_3| + |\mu_2|)\}^{-1}$. The initial coupling Hamiltonian H_c can be transformed by selective 180° rotations on the spins to either $2\pi C(|\mu_1|I_xS_x + |\mu_2|I_yS_y + |\mu_3|I_zS_z)$ or $-2\pi C(|\mu_1|I_xS_x + |\mu_2|I_yS_y + |\mu_3|I_zS_z)$. The maximum efficiency can be achieved by evolution under the Hamiltonian $\pm 2\pi C(|\mu_1|I_xS_x + |\mu_2|I_yS_y + |\mu_3|I_zS_z)$ for a duration $t/2$ followed by evolution under $\pm 2\pi C(|\mu_1|I_xS_x + |\mu_3|I_yS_y + |\mu_2|I_zS_z)$ for another period $t/2$, as depicted in Figs. 2A and A′.

The plot of the maximum achievable efficiency η^* versus the mixing time t also gives us the minimum time it takes to achieve a desired coherence transfer efficiency. We will refer to this plot as time-optimal pulse (TOP) curve. In Table 1, complete characterizations of TOP curves $\eta^*(t)$ are given for widely used coherence transfer elements, such as Cartesian in-phase to in-phase transfer ($I_x \to S_x$) as in refocused INEPT [4], coherence-order-selective in-phase to in-phase transfer ($I^- \to S^-$) as in sensitivity enhanced ICOS-CT experiments [5], Cartesian in-phase to anti-phase transfer ($I_x \to 2I_zS_x$) as in standard INEPT [6], coherence-order-selective in-phase to antiphase transfer ($I^- \to 2I_zS^-$) as in sensitivity enhanced COS-CT [7], and line-selective to line-selective transfer $I_xS_\beta \to I_\beta S_x$ and $I^-S_\beta \to I_\beta S^-$ as in TROSY [8,9]. Note that by fast local unitary transformations, I_x can be rapidly flipped to I_y or I_z, $I^- = I_x - \mathrm{i}I_y$ can be transformed to $I^+ = I_x + \mathrm{i}I_y$, and $I_\beta = \frac{1}{2} - I_z$ can be transformed to $I_\alpha = \frac{1}{2} + I_z$ and vice versa. Hence, each of the specific transfers stated in Table represents a whole class of locally equivalent transfers with the same TOP curves $\eta^*(t)$ and the same minimum time $t_{\min}$ to achieve complete transfer.

Examples of TOP curves are presented in Fig. 1 for four characteristic coupling tensors. Fig. 1A corresponds to the case of longitudinal, Ising-type coupling with $(\mu_1, \mu_2, \mu_3) = (0, 0, 1)$, which is characteristic for heteronuclear experiments [10,11]. Fig. 1B shows the case of planar coupling [12], also known as XY model [13] with $(\mu_1, \mu_2, \mu_3) = (0, 1, 1)$. Fig. 1C represents the generic case of homonuclear J coupling in isotropic solutions, also known as Heisenberg coupling with $(\mu_1, \mu_2, \mu_3) = (1, 1, 1)$. Finally, Fig. 1D corresponds to the case of dipolar coupling with $(\mu_1, \mu_2, \mu_3) = (-0.5, -0.5, 1)$, which is the dominant homonuclear coupling term in solid state NMR and also important in anisotropic solutions [14]. For example, in the case of the Cartesian transfer $I_x \to S_x$ under dipolar coupling (red TOP curve in Fig. 1D), the minimum time to achieve full transfer is $2/(3C) = 0.66/C$. In contrast, conventional pulse sequences [4,15] based solely on non-selective rf pulses require a 50% longer transfer time t.

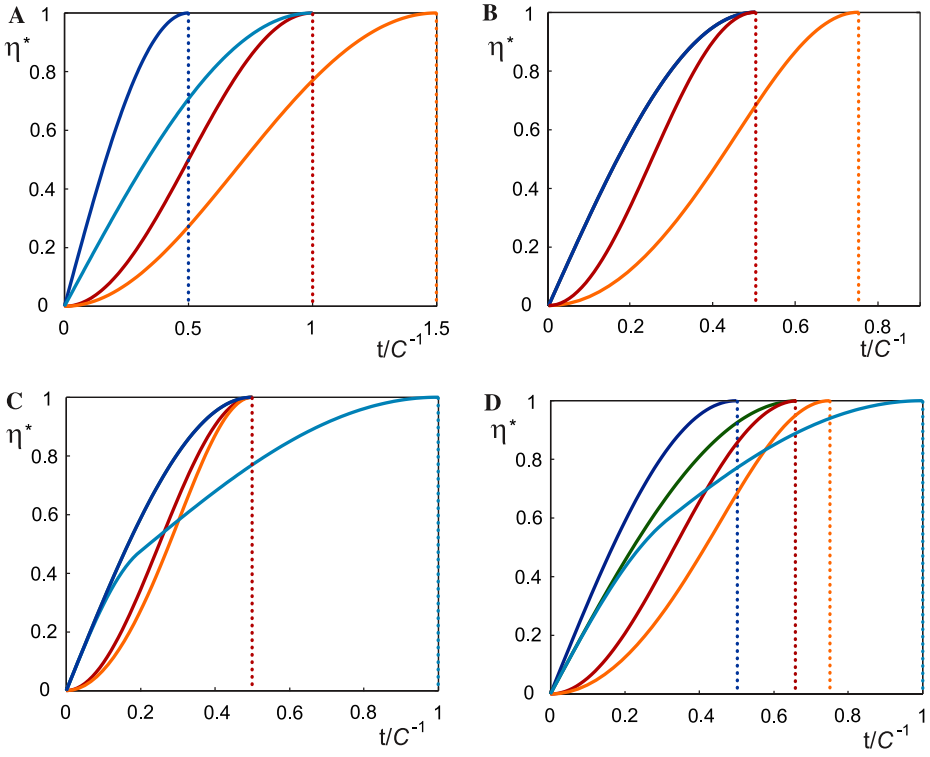

Fig. 1. Graphical representations of the TOP curves $\eta^*(t)$ for characteristic coherence transfers under (A) longitudinal (Ising) coupling with $(\mu_1,\mu_2,\mu_3)=(0,0,1)$, (B) planar coupling with $(\mu_1,\mu_2,\mu_3)=(0,1,1)$, (C) isotropic (Heisenberg) coupling with $(\mu_1,\mu_2,\mu_3)=(1,1,1)$, and (D) dipolar coupling with $(\mu_1,\mu_2,\mu_3)=(-0.5,-0.5,1)$. The curves represent the transfers $I_x\to S_x$ (red), $I^-\to S^-$ (orange), $I_x\to 2I_zS_x$ (dark blue), $I^-\to 2I_zS^-$ (light blue), $I_xS_\beta\to I_\beta S_x$, and $I^-S_\beta\to I_\beta S^-$ (green). Dark blue curves are overlapping with green curves in (A), (B), and (C), and with the light blue curve in (B). The dotted vertical lines indicate the minimum times $t_{\min}$ to achieve full transfers.

From Table 1 it follows that $t_{\min}(I_x\to S_x)=t_{\min}(I_xS_\beta\to I_\beta S_x)=t_{\min}(I^-S_\beta\to I_\beta S^-)$ and

$$t_{\min}(I_x\to 2I_zS_x)\leqslant t_{\min}(I_x\to S_x)\leqslant t_{\min}(I^-\to 2I_zS^-)\leqslant t_{\min}(I^-\to S^-)$$

if $|\mu_2|+|\mu_3|\geqslant 5|\mu_1|$ (cf. Figs. 1A and B), else (cf. Fig. 1C and D)

$$t_{\min}(I_x\to 2I_zS_x)\leqslant t_{\min}(I_x\to S_x)\leqslant t_{\min}(I^-\to S^-)\leqslant t_{\min}(I^-\to 2I_zS^-).$$

In Figs. 1C and D, the characteristic shape of the light blue TOP curves for the transfer $I^-\to 2I_zS^-$ results from the need to refocus the I_zS_z part of the coupling term, for details see Appendix A. Schematic representation of time optimal pulse sequences achieving the transfer limits are shown in Fig. 2.

3. Experimental

For practical NMR applications, the required selective manipulations of spins are most straightforward to implement in heteronuclear spin systems, which implies the weak coupling limit (Ising coupling) [10]. For homonuclear spin systems with general coupling tensors, rapid selective manipulation of spins is possible if the resonance frequencies of the spins of interest are well separated. The physical limits of coherence transfer efficiency in a given time will motivate the development of relatively straightforward pulse sequence elements (represented by boxes in Figs. 2A′–E′) for suppressing chemical shifts for given frequency ranges of practical interest to approach an effective coupling Hamiltonian of the form $\pm 2\pi C(|\mu_1|I_xS_x+|\mu_3|I_yS_y+|\mu_2|I_zS_z)$, as required by the time-optimal pulse sequences (cf. gray boxes in Figs. 2A′–E′).

To experimentally demonstrate an example of a non-trivial optimal coherence transfer sequence, we implemented the transfer $I^-\to S^-$ for an effective Hamiltonian of the form given in Eq. (1) with $C=10.8$ Hz and $(\mu_1,\mu_2,\mu_3)=(0.03,0.88,0.88)$. Homonuclear, spins I and S were represented by the H5 and H6 proton spins of cytosine in an anisotropic solvent consisting of filamentous Pf1 phage in 90% H_2O and 10% D_2O [15,16]. The phage concentration was adjusted such that the residual dipolar coupling constant D between I and S was the negative of the scalar coupling constant $J=7.2$ Hz. At a magnetic field of 14.1 Tesla, the transmitter frequency was set in the center of the two resonances, resulting in offset frequencies $\nu_I=459$ Hz and $\nu_S=-459$ Hz with a free evolution Hamiltonian of the form

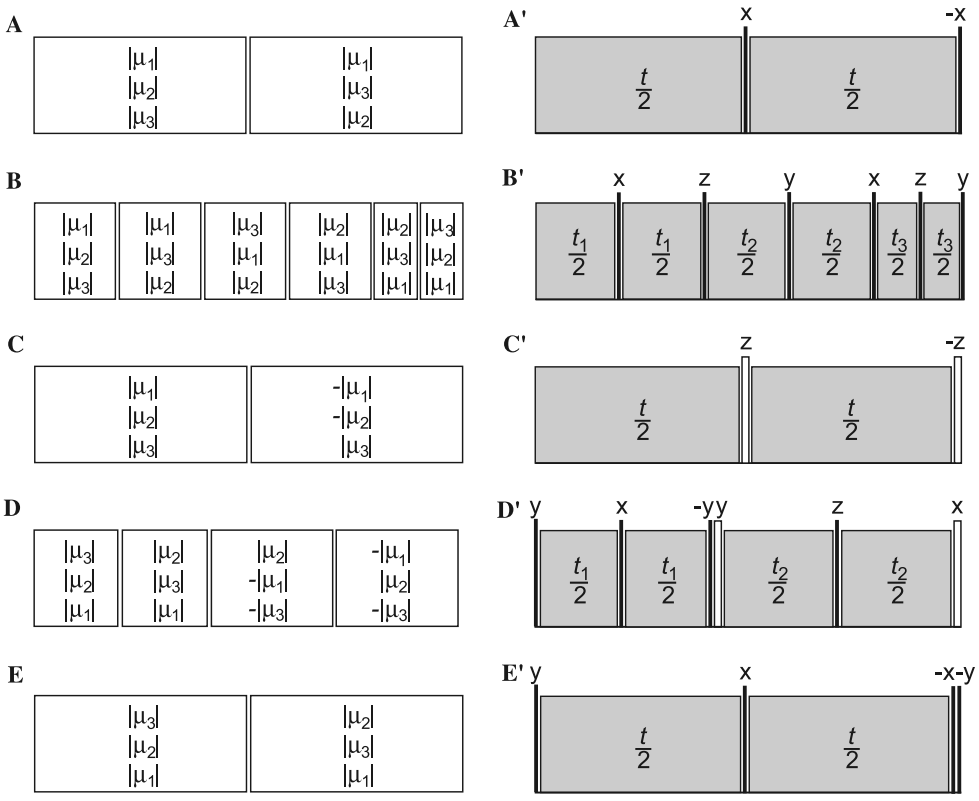

Fig. 2. Schematic representation of TOP sequences achieving the physical limit of transfer efficiency $\eta^*(t)$ in a given time t for the transfers $I_x \to S_x$ (A,A′), $I^- \to S^-$ (B,B′), $I_x \to 2I_zS_x$ (C,C′), $I^- \to 2I_zS^-$ (D,D′), $I_xS_\beta \to I_\beta S_x$, and $I^-S_\beta \to I_\beta S^-$ (E,E′). (A–E) The sequence of effective coupling Hamiltonians to be created during the sequence, where the triple in each box represents the prefactors of the bilinear coupling terms $2\pi CI_xS_x$, $2\pi CI_yS_y$, and $2\pi CI_zS_z$ in a toggling frame, respectively. For simplicity, here it is assumed that the initial coupling Hamiltonian H_c can be transformed by selective 180° rotations on the spins to $+2\pi C(|\mu_1|I_xS_x + |\mu_2|I_yS_y + |\mu_3|I_zS_z)$. (A′–E′) Schematic pulse sequences, where the gray boxes represent pulse sequence elements creating the effective Hamiltonian $2\pi C(|\mu_1|I_xS_x + |\mu_2|I_yS_y + |\mu_3|I_zS_z)$ (or $-2\pi C(|\mu_1|I_xS_x + |\mu_2|I_yS_y + |\mu_3|I_zS_z)$). The optimal durations t_1, t_2, and t_3 in B′ and t_1 and t_2 in D′ are specified in Appendix A. Narrow and wide bars represent 90° and 180° pulses, respectively. Solid bars represent non-selective pulses and open bars represent spin-selective pulses.

$$\mathscr{H} = 2\pi\nu_I\ (I_x - S_x) + 2\pi C\ (I_yS_y + I_zS_z)$$

with $C = J - D/2 = 10.8$ Hz, where we have labeled the axes such that the convention $|\mu_3| \geqslant |\mu_2| \geqslant |\mu_1|$ is fulfilled (cf. Eq. (1)). To eliminate the offset terms, we used a modified Carr–Purcell sequence [17–19] with a rf amplitude $-\gamma B_1/(2\pi)$ of 31.2 kHz and delays Δ of 264 μs which results in an effective Hamiltonian

$$\mathscr{H}_{\text{eff}} = 2\pi C\,(0.03\ I_xS_x + 0.88\ I_yS_y + 0.88\ I_zS_z). \qquad (6)$$

Given this effective Hamiltonian, the optimal pulse sequence for the transfer $I^- \to S^-$ was implemented. According to Table 1, the minimum time to achieve full transfer $(\eta = 1)$ is given by $t_{\min} = 3\{2C(|\mu_3| + |\mu_2| + |\mu_1|)\}^{-1} = 77.6$ ms and for a given total transfer time $t \leqslant t_{\min}$, the maximum possible transfer efficiency $\eta^*(t)$ is given by

$$\eta^*(t) = \sin(\pi Ca)\sin(\pi Cb) \qquad (7)$$

(cf. solid curve in Fig. 3A) with $(a + 2b)/t = |\mu_3| + |\mu_2| + |\mu_1| = 1.79$ and $\tan(\pi Ca) = 2\tan(\pi Cb)$.

In the general case where $\mu_1 \neq \mu_2 \neq \mu_3$, the optimal sequence of toggling frame Hamiltonians shown in Fig. 2B consists of six periods which can be realized by the pulse sequence given in Fig. 2B′. In the present case where $\mu_2 = \mu_3$, the general sequence of toggling frame Hamiltonians reduces to only three distinct periods with $\pm 2\pi C(|\mu_1|I_xS_x + |\mu_2|I_yS_y + |\mu_3|I_zS_z)$ for time t_1, $\pm 2\pi C(|\mu_3|I_xS_x + |\mu_1|I_yS_y + |\mu_2|I_zS_z)$ for time t_2, and $\pm 2\pi C(|\mu_2|I_xS_x + |\mu_3|I_yS_y + |\mu_1|I_zS_z)$ for time t_3. The corresponding pulse sequence can be simplified to $t_1 - (90°_z) - t_2 - (90°_{-z}90°_y) - t_3 - (90°_{-y})$. Note that due to the definition of the frame of reference, such that $|\mu_3| \geqslant |\mu_2| \geqslant |\mu_1|$ (cf. Eq. (1)), the $90°_y$ and $90°_z$ pulses correspond to $90°_x$ and $90°_y$ pulses in the usual rotating frame of reference. For any total time $t \leqslant t_{\min}$, the optimal durations $t_1 = t_2$ and t_3 are determined uniquely by the conditions $t_1 + t_2 + t_3 = t$ and $\tan(\pi Ca) = 2\tan(\pi Cb)$, where $a = (|\mu_2| + |\mu_3|)\,t_2 + |\mu_1|t_3$ and $b = |\mu_1|t_2 + (|\mu_2| + |\mu_3|)(t_2 + t_3)/2$ (cf. solid curves in Fig. 3B and Appendix A).

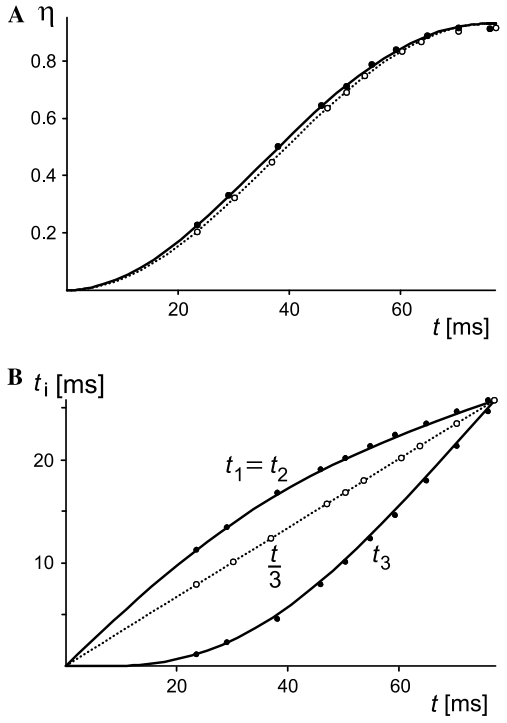

Fig. 3. (A) Comparison of transfer efficiencies $\eta(T)$ for the in-phase coherence-order selective coherence transfer $I^- \rightarrow S^-$. Solid curve and filled circles correspond to the theoretical (cf. Eq. (7)) and experimental transfer efficiency of the optimal pulse sequence for a non-isotropic effective Hamiltonian of the form $\mathscr{H}_{\text{eff}} = 2\pi\ 10.8$ Hz $(0.03\ I_xS_x + 0.88\ I_yS_y + 0.88\ I_zS_z)$ as a function of the total transfer time t. The dotted curve and open circles represent the case of isotropic mixing. To take into account small experimental relaxation losses, the theoretical curves were multiplied by an exponential damping function $\exp\{-t/T_d\}$ with $T_d = 1.06$ s. (B) Optimal durations t_1, t_2, and t_3 (solid curves) and the durations $t_1 = t_2 = t_3 = t/3$ of an isotropic mixing sequence (dotted line). The filled and open circles correspond to actual mixing periods t_i used in the experiments, where the time resolution was limited to multiples of 1.12 ms, corresponding to a single XY-4 cycle [17], i.e., one fourth of complete a complete XY-16 cycle [18].

To record experimental transfer efficiency curves $\eta(t)$ for the transfer $I^- \rightarrow S^-$ in the rotating frame, the initial density operator $\rho_o = I_x$ was prepared by selectively saturating spin S and by applying a hard $90°_y$ pulse to the thermal equilibrium spin I polarization. The solvent signal (H_2O) was suppressed by a combination of presaturation and pulsed field gradients. Before application of the transfer sequence, I_x was dephased by a pulsed field gradient. After the actual coherence transfer step, a refocusing gradient of opposite sign was applied before the free induction decay was recorded. As only -1 quantum coherence is detected by the standard quadrature detection scheme, the integrated intensity of the S resonance corresponds to the experimental transfer amplitude for $I^- \rightarrow S^-$. Fig. 3A shows the theoretical (solid line) and experimental (solid circles) transfer efficiency of the optimal pulse sequence as a function of t. For comparison, the dotted curve and open circles shows the theoretical and experimental transfer efficiency

$$\eta^{\text{IM}}(t) = \sin^2(\pi C\{\mu_1 + \mu_2 + \mu_3\}t/3)$$

of an isotropic mixing sequence with $t_1 = t_2 = t_3 = t/3$ [5,20–22] applied to the effective Hamiltonian in Eq. (6). In the limit of short transfer times, the optimal mixing sequence provides a gain of more than 11% compared to isotropic mixing. As the transfer time t is nearing $t_{\min}$, the optimal transfer sequence approaches the isotropic mixing sequence with $t_i = t/3$ (cf. Fig. 3B).

4. Conclusion

If no constraint is placed on the mixing time, the maximum achievable efficiency and pulse designs for the transfers considered in this paper are known [3,23,24]. However, for any specified mixing time t, we for the first time derive physical limits on the efficiency of coherence transfer between coupled spins 1/2 under general coupling tensors. Furthermore, we give shortest pulse sequences which achieve this maximum efficiency. The solution of this problem, besides being of fundamental interest in magnetic resonance, gives the best experimental designs for multidimensional NMR experiments where mixing times have to be curtailed due to relaxation losses. It is important to note that we have made no attempts in this paper to exploit the structure of relaxation. In our recent work, we have shown that in the presence of differential relaxation rates, it is possible to increase coherence transfer efficiency over one obtained by just reducing the mixing time [25–27]. However, in many practical applications, no differential relaxation exists or limited information about relaxation is available. With the development of methods which give unitary bounds on coherence transfer efficiencies in multiple spin topologies [3,23], it is of interest to extend the results of this paper to compute the minimum time and the corresponding pulse sequences to achieve these bounds in larger spin systems. For example, these include general I_nS spin systems (e.g., methylene or methyl groups in side chains of proteins) and chains of coupled heteronuclear or homonuclear spins (e.g., in protein backbone or side chain experiments). The techniques presented in this paper for computing limits of coherence transfer efficiency by first characterizing the set of unitary transformations that can be synthesized in a specified time forms a systematic methodology for approaching these problems. Furthermore, such a characterization of unitary evolutions is of great significance in the general area of quantum information processing. This allows to address problems like characterizing the difficulty of generating a desired state in coupled spin topologies or finding the minimum time to transfer an unknown state completely between two coupled spins under a given coupling tensor.

Appendix A

Given the coupling Hamiltonian $\mathscr{H}_c$ in Eq. (1), we can by local rotations on the spins, transform it to either (not both) $2\pi C(|\mu_1|I_xS_x + |\mu_2|I_yS_y + |\mu_3|I_zS_z)$ or $-2\pi C(|\mu_1|I_xS_x + |\mu_2|I_yS_y + |\mu_3|I_zS_z)$. The computations for maximum achievable efficiency are the same starting from either of these transformed Hamiltonians. Therefore, without loss of generality, we will assume, in the following that the coupling Hamiltonian is

$\mathscr{H}_c = 2\pi C(|\mu_1|I_xS_x + |\mu_2|I_yS_y + |\mu_3|I_zS_z)$.

1. First we consider the transfer

$I^- \to S^-$.

To derive the optimal efficiency for this transfer, we state two lemmas that we will use in the course of the proof.

Lemma 1.

Let $p = \begin{bmatrix} 1 \\ -i \\ 0 \end{bmatrix}$, $\Sigma = \begin{bmatrix} a_1 & 0 & 0 \\ 0 & a_2 & 0 \\ 0 & 0 & a_3 \end{bmatrix}$, $a_i \geqslant 0$ and U, V, *three-dimensional rotation matrices. The maximum value of* $\|p^\dagger U\Sigma Vp\|$ *is the sum of the largest two diagonal entries of* Σ.

Proof. Let

$$\Lambda = \begin{bmatrix} \sqrt{a_1} & 0 & 0 \\ 0 & \sqrt{a_2} & 0 \\ 0 & 0 & \sqrt{a_3} \end{bmatrix}.$$

By definition $\Sigma = \Lambda^\dagger\Lambda$. Using Cauchy Schwartz inequality $\|p^\dagger U\Sigma Vp\| \leqslant \|\Lambda Vp\|\,\|\Lambda Up\|$. Observe, the maximum value of $\|\Lambda Vp\|$ is $\sqrt{a_k + a_l}$, where a_k and a_l are the two largest diagonal entries of Σ. Therefore, $\|p^\dagger U\Sigma Vp\| \leqslant a^k + a_l$. For appropriate choice of U and V, this upper bound is achieved (For example, in the case $a_1 \geqslant a_2 \geqslant a_3$, the bound is achieved for U and V identity). □.

Lemma 2. *Consider the function* $f(\gamma,\beta,\alpha) = \sin(C\pi\gamma t)\sin(C\pi\beta t) + \sin(C\pi\gamma t)\sin(C\pi\alpha t)$, *where* $\gamma,\beta,\alpha \geqslant 0$. *For a fixed value of* $(\gamma+\beta+\alpha)t \leqslant 3/(2C)$, *the maximum value of* $f(\gamma,\beta,\alpha)$ *is* $2\sin(C\pi a)\sin(C\pi b)$, *where* $a + 2b = (\alpha+\beta+\gamma)t$ *and* $\tan(C\pi a) = 2\tan(C\pi b)$. *The maximum is achieved when* $\alpha = \beta$.

This is a constrained optimization problem, which can be solved by introducing the Lagrange multiplier λ and maximizing

$$H(\gamma,\beta,\alpha,\lambda) = \sin(C\pi\gamma t)\sin(C\pi\beta t) + \sin(C\pi\gamma t)\sin(C\pi\alpha t) + \lambda(\gamma+\beta+\alpha)t.$$

The necessary condition for optimality gives $\frac{\partial H}{\partial\gamma} = 0$, $\frac{\partial H}{\partial\beta} = 0$, and $\frac{\partial H}{\partial\alpha} = 0$, which imply, respectively, that

$$\pi C(\cos(C\pi\gamma t)\sin(C\pi\beta t) + \cos(C\pi\gamma t)\sin(C\pi\alpha t)) + \lambda = 0, \tag{A.1}$$

$$\pi C(\sin(C\pi\gamma t)\cos(C\pi\beta t)) + \lambda = 0, \tag{A.2}$$

$$\pi C(\sin(C\pi\gamma t)\cos(C\pi\alpha t)) + \lambda = 0. \tag{A.3}$$

From Eqs. (A.2) and (A.3), we obtain that either $\sin(C\pi\gamma t) = 0$ or $\cos(C\pi\beta t) = \cos(C\pi\alpha t)$. The first condition does not give a maxima as it makes f identically zero. The second condition implies

$$C\pi\beta t = 2m\pi + C\pi\alpha t. \tag{A.4}$$

Since $\beta,\alpha \geqslant 0$ and $t(\alpha+\beta) \leqslant 3/(2C)$, condition (A.4) is only satisfied for $m = 0$. Therefore, $\alpha = \beta$. Now substituting this in (A.1) and using the Eqs. (A.1) and (A.2), we get the desired result. □

We now seek to maximize the expression $|\mathrm{tr}(S^+U(t)I^-U^\dagger(t))|$. Let $\mathfrak{s}$ denote the subspace spanned by the orthonormal basis $\{S_x, S_y, S_z\}$ and $\mathfrak{i}$ denote the subspace spanned by the orthonormal basis $\{I_x, I_y, I_z\}$. We represent the starting operator $\frac{1}{\sqrt{2}}(I_x - \mathrm{i}I_y)$ as a column vector $p = \frac{1}{\sqrt{2}}[1\ -i\ 0]^{\mathrm{T}}$ in $\mathfrak{i}$. The action $I^- \to K_1I^-K_1^\dagger$ can then be represented as $p \to Vp$, where V is an orthogonal matrix. Similarly the operator $S^+ = \frac{(S_x+\mathrm{i}S_y)}{\sqrt{2}}$ is represented as a column vector $\frac{1}{\sqrt{2}}[1\ i\ 0]^{\mathrm{T}}$ in $\mathfrak{s}$. Using the characterization of $U(t) = K_1A(t)K_2$ in Eq. (2), we observe that $|\mathrm{tr}(S^+U(t)I^-U^\dagger(t))|$ can be written as $\|p^\dagger U\Sigma Vp\|$, where U and V are real orthogonal matrices and

$$\Sigma = \begin{bmatrix} \sin(C\pi\gamma t)\sin(C\pi\beta t) & 0 & 0 \\ 0 & \sin(C\pi\gamma t)\sin(C\pi\alpha t) & 0 \\ 0 & 0 & \sin(C\pi\alpha t)\sin(C\pi\beta t) \end{bmatrix},$$

where $\alpha+\beta+\gamma = (|\mu_1| + |\mu_2| + |\mu_3|)t$. Now using Lemma 1 and 2, we obtain that the maximum efficiency is given by $\sin(\pi Ca)\sin(\pi Cb)$, where $a + 2b = (|\mu_1| + |\mu_2| + |\mu_3|)t$ and $\frac{\tan(\pi Ca)}{\tan(\pi Cb)} = 2$.

In practice, we can achieve this efficiency by evolving the Hamiltonian $2\pi C(|\mu_1|I_xS_x + |\mu_2|I_yS_y + |\mu_3|I_zS_z)$, followed by the Hamiltonian $2\pi C(|\mu_1|I_xS_x + |\mu_3|I_yS_y + |\mu_2|I_zS_z)$ each for time $t_1/2$. This is followed by evolution of Hamiltonians $2\pi C(|\mu_3|I_xS_x + |\mu_1|I_yS_y + |\mu_2|I_zS_z)$, $2\pi C(|\mu_2|I_xS_x + |\mu_1|I_yS_y + |\mu_3|I_zS_z)$, each of duration $t_2/2$, followed by $2\pi C(|\mu_2|I_xS_x + |\mu_3|I_yS_y + |\mu_1|I_zS_z)$, $2\pi C(|\mu_3|I_xS_x + |\mu_2|I_yS_y + |\mu_1|I_zS_z)$, each of duration $t_3/2$. Observe that $t_1 + t_2 + t_3 = t$ and for the optimal sequence $t_1 = t_2$ and $\frac{\tan(\pi Ca)}{\tan(\pi Cb)} = 2$, where $a = (|\mu_2| + |\mu_3|)t_2 + |\mu_1|t_3$ and $b = (|\mu_2| + |\mu_3|)(t_2 + t_3)/2 + |\mu_1|t_2$. These three relations determine t_1, t_2, and t_3 uniquely. See Fig. 2B.

2. Now we consider the transfer

$I_x \to 2I_zS_x$.

Observe the efficiency of this transfer is the same as that of the transfer $I_x \to 2I_yS_z$, as a local rotation on spin I and S is sufficient to go between the operators $2I_yS_z$ and $2I_zS_x$. This local transformation is assumed to take negligible time. We now compute the unitary

evolution $U(t)$ that maximizes $|\mathrm{tr}(2I_yS_zU(t)I_xU^\dagger(t))|$. Based on the characterization of $U(t) = K_1A(t)K_2$ as in Eq. (2), consider the case when K_2 is identity. In this case

$$A(t)I_xA^\dagger(t) = \sin(\pi C\gamma t)\cos(\pi C\beta t)\ 2I_yS_z + \sin(\pi C\gamma t) \times \sin(\pi C\beta t)\ S_x.$$

The maximum projection of $K_1A(t)I_xA^\dagger(t)K_1^\dagger$ onto $2I_yS_z$ is then $\sin(\pi C\gamma t)\cos(\pi C\beta t)$ and is achieved when K_1 is an identity transformation. This value $\sin(\pi C\gamma t)\cos(\pi C\beta t)$ is maximized for $\beta = 0$ and γt as large as possible (as long as $\gamma t \leqslant 1/(2\pi C)$). From (2), the vector (α,β,γ) lies in the convex cone generated by vectors (μ_1,μ_2,μ_3), $(\mu_1,-\mu_2,-\mu_3)$, $(-\mu_1,-\mu_2,\mu_3)$, $(-\mu_1,\mu_2,-\mu_3)$ and their various permutations. Under these constraints the optimal values of γ and β are $|\mu_3|$ and 0, respectively. The maximum efficiency is $\sin(\pi C|\mu_3|t)$. For the local unitary transformation K_2 other than identity $K_2I_xK_2^\dagger = m_1I_x + m_2I_y + m_3I_z$, where $\sum_i m_i^2 = 1$. Each of these single spin operators have the maximum transfer efficiency of $\sin(\pi C|\mu_3|t)$ to the target state $2I_yS_z$ by choice of suitable $A(t)$ and K_1 as described above. There is no gain by having K_2 other than identity and we obtain the maximum efficiency when $K_2 = 1$. The maximum efficiency can be achieved by evolution under the Hamiltonian $2\pi C(|\mu_1|I_xS_x + |\mu_2|I_yS_y + |\mu_3|I_zS_z)$ for $t/2$ amount of time followed by evolution under $2\pi C(-|\mu_1|I_xS_x - |\mu_2|I_yS_y + |\mu_3|I_zS_z)$ for another $\frac{t}{2}$ as depicted in Fig. 2C.

3. Consider the transfer

$$\frac{I^\pm}{\sqrt{2}} \to \sqrt{2}I_zS^\pm.$$

Consider the action of $A(t)$ in Eq. (2) on the operator I^+. We obtain by direct computation that

$$|\mathrm{tr}(I_zS^-AI^+A^\dagger)| = \frac{\cos(\pi Ct\gamma)}{2}(\sin(\pi Ct\alpha) + \sin(\pi Ct\beta)).$$

We would like to have $\gamma = 0$ and α and β large, but we know that (α,β,γ) lies in a convex cone as described in Theorem 1. Under these restrictions then, $\frac{\cos(\pi Ct\gamma)}{2}(\sin(\pi Ct\alpha) + \sin(\pi Ct\beta))$ is maximized for $\alpha = \beta$. To maximize α and β, we evolve the Hamiltonian $2\pi C(|\mu_2|I_xS_x + |\mu_3|I_yS_y + |\mu_1|I_zS_z)$ for $\frac{t_1}{2}$ units of time followed by evolution of $2\pi C\,(|\mu_3|I_xS_x + |\mu_2|I_yS_y + |\mu_1|I_zS_z)$ for another $\frac{t_1}{2}$ units of time. This produces an effective Hamiltonian $2\pi Ct_1(\frac{|\mu_2|+|\mu_3|}{2}(I_xS_x + I_yS_y) + |\mu_1|I_zS_z)$. To reduce γ, we evolve the Hamiltonian $2\pi C(|\mu_2|I_xS_x - |\mu_1|I_yS_y - |\mu_3|I_zS_z)$ followed by $2\pi C(-|\mu_1|I_xS_x + |\mu_2|I_y$-$C(-|\mu_1|I_xS_x + |\mu_2|I_yS_y - |\mu_3|I_zS_z)$ for $\frac{t_2}{2}$ units of time each. See Fig. 2D. This produces an effective Hamiltonian $2\pi Ct_2(\frac{|\mu_2|-|\mu_1|}{2}(I_xS_x + I_yS_y) - |\mu_3|I_zS_z)$. Given $t_1 + t_2 = t$, we can now substitute the value of α, β, and γ to find that $\cos(\pi Ct\gamma)\sin(\pi Ct\alpha)$ reduces to $\cos(\pi Ct\gamma)\sin(\frac{\pi}{2}Ct(|\mu_3| + |\mu_2| - |\mu_1| + \gamma))$. We can now maximize this expression for $|\gamma| \leqslant |\mu_3|$. This is the maximum efficiency. As before nothing is gained by having K_1 and K_2 other than identity transformation. The efficiency of $\frac{I^-}{\sqrt{2}} \to \sqrt{2}I_zS^-$ is the same.

4. Next, we consider the transfer

$$\sqrt{2}I_xS_\alpha \to \sqrt{2}I_\alpha S_x.$$

Consider the action of $A(t)$ in Eq. (2) on the operator $\sqrt{2}I_xS_\alpha$. Let $\mathfrak{s}$ denote the subspace spanned by the orthonormal basis $\{\sqrt{2}I_\alpha S_x, \sqrt{2}I_\alpha S_y, \sqrt{2}I_\alpha S_z\}$ and let P_s denote the projection onto this space. Then we obtain

$$P_s(A(t)\ \sqrt{2}I_xS_\alpha\ A^\dagger(t)) = \frac{\sin(\pi Ct\alpha) + \sin(\pi Ct\beta)}{2}.$$

Note $|P_s(A\ I_xS_\alpha\ A^\dagger)|$ is all we need to maximize, as then by a suitable local unitary K_1, we can rotate this projection onto $I_\alpha S_x$. Maximizing the above expression then gives $\alpha = \beta = \frac{|\mu_3|+|\mu_2|}{2}$. In practice we can achieve this efficiency by evolving the Hamiltonian $2\pi C(|\mu_3|I_xS_x + |\mu_2|I_yS_y + |\mu_1|I_zS_z)$ for $t/2$ amount of time followed by the evolution of the Hamiltonian $2\pi C(|\mu_2|I_x\ S_x + |\mu_3|I_y$-$S_y + |\mu_1|I_zS_z)$ for time $t/2$. See Fig. 2E. Note, we have in the above discussion taken K_2 as identity transformation. In general if K_2 is not zero, starting from the initial operator I_xS_α, it will create $\sum_{pq} m_pn_q(\frac{I_p}{2} + I_pS_q)$, where $\sum_p m_p^2 = 1$ and $\sum_q n_q^2 = 1$ and $p,q \in \{x,y,z\}$. Since for the term $(\frac{I_p}{2} + I_pS_q)$, the maximum transfer efficiency to the subspace $\mathfrak{s}$ is bounded by $\sin(\frac{\pi}{2}Ct(|\mu_2| + |\mu_3|))$, the total maximum efficiency is achieved for K_2, an identity transformation.

5. The maximal efficiency for the transfer

$$I^\pm S_\alpha \to I_\alpha S^\pm$$

is the same and can be derived as above.

References

[1] N. Khaneja, Geometric control in classical and quantum systems, Ph.D. Thesis, Harvard University, 2000.

[2] N. Khaneja, R.W. Brockett, S.J. Glaser, Time optimal control in spin systems, Phys. Rev. A. 63 (2001) 032308.

[3] S.J. Glaser, T. Schulte-Herbrüggen, M. Sieveking, O. Schedletzky, N.C. Nielsen, O.W. Sørensen, C. Griesinger, Unitary control in quantum ensembles, maximizing signal intensity in coherent spectroscopy, Science 208 (1998) 421–424.

[4] D.P. Burum, R.R. Ernst, Net polarization transfer via a *J*-ordered state for signal enhancement of low-sensitivity nuclei, J. Magn. Reson. 39 (1980) 163–168.

[5] M. Sattler, P. Schmidt, J. Schleucher, O. Schedletzky, S.J. Glaser, C. Griesinger, Novel pulse sequences with sensitivity enhancement for in-phase coherence transfer employing pulsed field gradients, J. Magn. Reson. B. 108 (1995) 235–242.

[6] G.A. Morris, R. Freeman, Enhancement of nuclear magnetic resonance signals by polarization transfer, J. Am. Chem. Soc. 101 (1979) 760–762.

[7] J. Schleucher, M. Schwendinger, M. Sattler, P. Schmidt, O. Schedletzky, S.J. Glaser, O.W. Sørensen, C. Griesinger, A general enhancement scheme in heteronuclear multidimensional NMR

employing pulsed field gradients, J. Biomol. NMR 4 (1994) 301–306.
[8] K. Pervushin, R. Riek, G. Wider, K. Wüthrich, Transverse relaxation-optimized spectroscopy, Proc. Natl. Acad. Sci. USA 94 (1997) 12366–12371.
[9] M. Salzmann, K. Pervushin, G. Wider, H. Senn, K. Wüthrich, Proc. Natl. Acad. Sci. USA 95 (1998) 13585–13590.
[10] R.R. Ernst, G. Bodenhausen, A. Wokaun, Principles of Nuclear Magnetic Resonance in One and Two Dimensions, Clarendon Press, Oxford, 1987.
[11] S.J. Glaser, Coupling topology dependence of polarization-transfer efficiency in TOCSY and TACSY experiments, J. Magn. Reson. A 104 (1993) 283–301.
[12] T. Schulte-Herbrüggen, Z.L. Mádi, O.W. Sørensen, R.R. Ernst, Reduction of multiplet complexity in COSY-type NMR spectra, the bilinear and planar COSY experiment, Mol. Phys. 72 (1991) 847–871.
[13] E.H. Lieb, T. Schultz, D.C. Mattis, Antiferromagnetic chain, Ann. Phys. 16 (1961) 407–466.
[14] N. Tjandra, A. Bax, Direct measurement of distances and angles in biomolecules by NMR in a dilute liquid crystalline medium, Science 278 (1997) 1111–1114.
[15] F. Kramer, S.J. Glaser, Efficiency of Homonuclear Hartmann–Hahn and COSY-type mixing sequences in the presence of scalar and residual dipolar couplings, J. Magn. Reson. 155 (2002) 83–91.
[16] M.R. Hansen, P. Hanson, A. Pardi, Filamentous bacteriophage for aligning RNA, DNA, and proteins for measurement of Nuclear Magnetic Resonance dipolar coupling interactions, Methods Enzymol. 317 (2002) 220–240.
[17] T. Gullion, D.B. Baker, M.S. Conradi, New, compensated Carr–Purcell sequences, J. Magn. Reson. 89 (1990) 479–484.
[18] M.J. Lizak, T. Gullion, M.S. Conradi, Measurement of like-spin dipole couplings, J. Magn. Reson. 91 (1991) 254–260.
[19] F. Kramer, W. Peti, C. Griesinger, S.J. Glaser, Optimized homonuclear Carr–Purcell-type dipolar mixing sequences, J. Magn. Reson. 149 (2001) 58–66.
[20] D.P. Weitekamp, J.R. Garbow, A. Pines, Determination of dipole coupling constants using heteronuclear multiple quantum NMR, J. Chem. Phys. 77 (1982) 2870–2883.
[21] P. Caravatti, L. Braunschweiler, R.R. Ernst, Heteronuclear correlation spectroscopy in rotating solids, Chem. Phys. Lett. 100 (1983) 305–310.
[22] S.J. Glaser, J.J. Quant, Homonuclear and heteronuclear Hartmann–Hahn transfer in isotropic liquids, in: W.S. Warren (Ed.), Advances in magnetic and optical resonance, 19, Academic Press, San Diego, 1995, pp. 59–252.
[23] O.W. Sørensen, Polarization transfer experiments in high-resolution NMR spectroscopy, Prog. NMR Spectrosc. 21 (1989) 503–569.
[24] T.S. Untidt, N.C. Nielsen, Analytical unitary bounds on quantum dynamics: Design of optimum NMR experiments in two-spin-1/2 systems, J. Chem. Phys. 113 (2000) 8464–8471.
[25] N. Khaneja, T. Reiss, B. Luy, S.J. Glaser, Optimal control of spin dynamics in the presence of relaxation, J. Magn. Reson. 162 (2003) 311–319.
[26] D. Stefanatos, N. Khaneja, S.J. Glaser, Optimal control of coupled spins in presence of longitudinal relaxation, Phys. Rev. A 69 (2004) 022319.
[27] N. Khaneja, B. Luy, S.J. Glaser, Boundary of quantum evolution in presence of decoherence, Proc. Natl. Acad. Sci. USA (2003) 13162–13166.